



AALBORG UNIVERSITY
DENMARK

Aalborg Universitet

The CardioSynchroGram

A method to visualize and quantify ventricular dyssynchrony

Melgaard, Jacob; Struijk, Johannes Jan; Kanters, Jørgen K.; Sørensen, Peter Lyngø; Graff, Claus

Published in:
Journal of Electrocardiology

DOI (link to publication from Publisher):
[10.1016/j.jelectrocard.2019.09.020](https://doi.org/10.1016/j.jelectrocard.2019.09.020)

Creative Commons License
CC BY-NC-ND 4.0

Publication date:
2019

Document Version
Accepted author manuscript, peer reviewed version

[Link to publication from Aalborg University](#)

Citation for published version (APA):
Melgaard, J., Struijk, J. J., Kanters, J. K., Sørensen, P. L., & Graff, C. (2019). The CardioSynchroGram: A method to visualize and quantify ventricular dyssynchrony. *Journal of Electrocardiology*, 57(supplement), S45-S50. Advance online publication. <https://doi.org/10.1016/j.jelectrocard.2019.09.020>

General rights

Copyright and moral rights for the publications made accessible in the public portal are retained by the authors and/or other copyright owners and it is a condition of accessing publications that users recognise and abide by the legal requirements associated with these rights.

- Users may download and print one copy of any publication from the public portal for the purpose of private study or research.
- You may not further distribute the material or use it for any profit-making activity or commercial gain
- You may freely distribute the URL identifying the publication in the public portal -

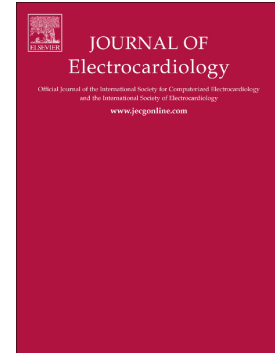
Take down policy

If you believe that this document breaches copyright please contact us at vbn@aub.aau.dk providing details, and we will remove access to the work immediately and investigate your claim.

Journal Pre-proof

The CardioSynchroGram: A method to visualize and quantify ventricular dyssynchrony

Jacob Melgaard, Johannes J. Struijk, Jørgen K. Kanters, Peter L. Sørensen, Claus Graff



PII: S0022-0736(19)30458-3

DOI: <https://doi.org/10.1016/j.jelectrocard.2019.09.020>

Reference: YJELC 52940

To appear in: *Journal of Electrocardiology*

Received date: 27 June 2019

Revised date: 18 September 2019

Accepted date: 25 September 2019

Please cite this article as: J. Melgaard, J.J. Struijk, J.K. Kanters, et al., The CardioSynchroGram: A method to visualize and quantify ventricular dyssynchrony, *Journal of Electrocardiology*(2018), <https://doi.org/10.1016/j.jelectrocard.2019.09.020>

This is a PDF file of an article that has undergone enhancements after acceptance, such as the addition of a cover page and metadata, and formatting for readability, but it is not yet the definitive version of record. This version will undergo additional copyediting, typesetting and review before it is published in its final form, but we are providing this version to give early visibility of the article. Please note that, during the production process, errors may be discovered which could affect the content, and all legal disclaimers that apply to the journal pertain.

© 2018 Published by Elsevier.

The CardioSynchroGram: A Method to Visualize and Quantify Ventricular Dyssynchrony

Jacob Melgaard¹, Johannes J. Struijk¹, Jørgen K. Kanters², Peter L. Sørensen¹ and Claus Graff¹

¹CardioTech Research Group, Department of Health Science and Technology, Aalborg University, Aalborg, Denmark.

²Laboratory of Experimental Cardiology, Department of Biomedical Sciences, University of Copenhagen, Denmark.

Presenting Author:

Jacob Melgaard
Dept. of Health Science and Technology
Aalborg University
Fredrik Bajers Vej 7D
9220 Aalborg OE
Denmark
jm@hst.aau.dk
Tel: +45 6133 6143

Introduction

Cardiac resynchronization therapy (CRT) is a treatment option for patients with reduced left ventricular (LV) function, symptomatic heart failure (HF), and wide QRS on the electrocardiogram (ECG). CRT can improve LV function and reduce heart failure symptoms, thereby improving not only quality of life, but also reducing HF related hospitalization and mortality [1]. The most common conduction disorder in HF is Left Bundle Branch Block (LBBB) which occurs in up to 30 % of advanced heart failure patients [2]. Recommendations for the interpretation of the ECG use QRS-duration and –notching as markers of LBBB [3], and clinical guidelines recommend that HF patients with reduced Ejection Fraction (HFrEF) and LBBB are treated with CRT [4], [5]. However, up to 40% of patients treated with a CRT device do not respond to treatment [6]. Therefore, better markers of ventricular dyssynchrony are needed to predict response and select patients for CRT [7].

Methods proposed to assess electrical dyssynchrony include ECG imaging [8] and the so-called intrinsicoid deflection [9]. Both are related to the ‘intrinsic deflection’ first described in 1915 [10], where epicardial breakthrough (defined as when the activation wavefront reaches the epicardium) is associated with a negative deflection in an epicardial electrode located atop the tissue. This concept was extended with the intrinsicoid deflection (ID) in the surface ECG; the definition given by Del-Carpio Munoz et al. [9] is that ID is the onset of the main transition towards zero potential in a lead as an indication of epicardial breakthrough. In contrast, Ramanathan et al. [8] used body-surface potential maps recorded from 224 electrodes to model the unipolar epicardial electrograms, and defined the maximum negative slope, denoted $-dV/dt_{\max}$, as the ‘activation time’ (epicardial breakthrough) of each epicardial point.

We propose a novel method—the CardioSynchroGram (CSG)—to visualize and to quantify electrical (dys)synchrony within the QRS complex, based on principles similar to the activation time, although obtained from the standard clinical 12-lead ECG.

Methods

Derivation of the CardioSynchroGram (CSG)

In the following, we describe our physiological understanding of the Cardiosynchrogram. We consider epicardial breakthrough and intrinsic deflections in the setting of two (or more) opposing depolarizing wavefronts, as illustrated on a cross-section of the ventricles in figure 1A. Initial activation of the septum (t_1) is followed by simultaneous activation of both right and left ventricular free walls (t_2). When there is a large epicardial breakthrough in the right ventricular free wall (t_3), the imbalance of the electrical forces is maximal, giving rise to the maximum negative slope in V1 (and maximum positive slope in V6). Next, epicardial breakthrough occurs at the apex and the left ventricular free wall (t_4), causing large loss of activation wavefront, and return of the potentials towards zero. This gives rise to the maximum negative slope in V6 (and maximum positive slope in V1). The latest activating parts of the heart are the basal areas and the right outflow tract (t_5), giving rise to a small r' wave in V1 and an S wave in V6. At t_6 , depolarization is complete and the stylistic normal variants of leads V1 and V6 are shown for reference. Because the colored clusters in the CSG represent the times and locations of epicardial breakthrough, we coin breakthrough times obtained from the cardiosynchrogram 'EpiTimes'.

There are two problems associated with assessment of epicardial breakthrough directly from the standard ECG, especially paper printouts. Mainly, it is difficult to assess both the timing and steepness across leads. Moreover, there is limited view in terms of full 3D activation. To circumvent these limitations, the following steps are taken to construct the CardioSynchroGram. 1) Compute the vectorcardiogram (VCG) based on a known transform, e.g. the inverse Dower [11] or Kors [12] transform; in this study, the Kors transform was used. 2) Define 36 virtual leads with 10 degree steps in each of the three anatomically perpendicular planes - transverse, frontal, and sagittal. 3) Generate ECGs for each of the virtual leads by projecting the VCG onto each of the virtual leads. 4) Compute the first derivative signal in each of the virtual leads. 5) Visualize the derivative values within the QRS complex as colored bands. All positive values are represented as white,

whereas the negative derivatives are coded from yellow to dark-blue proportional to the magnitude of their (negative) derivative values by a 64-step color mapping scheme ranging from just negative (yellow) to the maximum negative value (dark blue). The arrangement of color-coded bands makes it easy to compare timing across leads. We term this plot the CardioSynchroGram (Figure 3 C).

Simulation of Gross Activation Patterns

To validate the qualitative nature of the CardioSynchroGram, we conducted simulation studies of right and left bundle branch blocks using ECGsim [13] (www.ecgsim.org, release 3.0.0). ECGsim uses a heart and torso model consisting of fixed nodes, with a certain (adjustable) action potential defined for each node of the heart, and a transfer matrix from the heart to the body surface. In this study, the 'normal male' model of ECGsim was used. In this model, the ventricular geometry is defined by 257 nodes, and the torso is defined by 300 nodes. A forward transform matrix from the ventricular nodes to the torso nodes is defined based on geometry and tissue properties, and given this relation, the depolarization sequence of the ventricles are fitted from a 198-point measured body-surface potential map as described by Huiskamp and Oosterom [14] using a constrained minimization technique. In ECGsim, initial activating nodes and conduction velocities within the ventricles can be defined, such that depolarization time for all other nodes will be computed from a theoretical propagation. To simulate left bundle branch block (LBBB), we eliminated all initial activation points in the left ventricle but not those in the right ventricle, such that the activation of both ventricles started in the right ventricle. Right bundle branch block (RBBB) was thus simulated by removal of the right ventricular initial activation points. The simulated ECGs were exported, and the corresponding CardioSynchroGrams were computed from these ECGs. All activation times in ECGsim are absolute times, hence the true QRS duration must be found as the difference between the earliest endocardial activation and the latest epicardial breakthrough.

Simulation of Spatially Confined Local Delays

Temporal precision of the CardioSynchroGram was assessed on ECGs exported from ECGSim where spatially confined local activation delays were simulated at nine locations. We used the six nodes most directly below each of the precordial electrodes V1-V6, and in addition one node on the basal septum, one on the inferior aspect of the left ventricle (LV), and one on the superior aspect of LV. The nodes for each of the precordial leads were selected by computing the geometric center of the heart, and taking a straight line to each precordial electrode. The epicardial node closest to this line was selected. Then, one at a time each of the epicardial nodes were selected and the action potentials were delayed in an area with a radius of 20 mm around the selected node by 25 ms compared to the normal activation time. The QRS duration was not changed by any of the imposed delays; the repolarization time was also unaffected. The nine resulting ECGs were exported, and EpiTimes were calculated from the ECGs using the CardioSynchroGram in the following way. At each point in time the virtual lead with the most negative derivative was marked by a small white circle in the CSG (see fig. 2 and 3). These points indicate the position of epicardial breakthrough. We then computed the weighted average activation time and position within each delayed activation clusters (fig. 3) by weighing the time of occurrence and position of each white circle by its corresponding absolute negative derivative. That is, a yellow color corresponds to a small weight for that time point, and blue color corresponds to a large weight. The plane which showed the delay most clearly was used to mark onset and offset. The absolute activation times for each of the 9 delayed nodes were obtained from ECGsim, and compared with the EpiTimes from the CardioSynchrogram using a paired t-test.

Results

Simulation of Gross Activation Patterns

For reference, the isochrone map (ECGsim) and CardioSynchroGram from the standard case ('normal male') are shown in figure 2 panel A. On the ECGsim heart model, earliest activation occurs at 8 ms (LV endocardium), and the latest activation occurs at 96 ms (Right base); thus, the QRS duration is 88 ms. The

latest activation of the left ventricle is at 61 ms. On the transverse plane of the CardioSynchroGram, the main activation ends after 62 ms.

In the LBBB simulation, initial activation on the ECGsim heart model is at 19 ms, and the latest activation is at 198 ms, resulting in a QRS duration of 179 ms. The simulated ECG shows typical LBBB morphology with leads V1 to V3 having QS configurations with (absolute) amplitude > 3 mV, and V5 and V6 are positive and notched. The corresponding ECGsim isochrone map and the CardioSynchroGram is shown in figure 2 panel B. On the ECGsim heart model, septal activation travels in a posterolateral direction and is complete around 131 ms (left basal area of septum; found by marking the latest activating septal node and inspecting its onset). The right base is fully activated at 153 ms, with the LV free wall being the only active part for the remainder of the QRS duration. On the CardioSynchroGram, there is a posterior-leftward activation until 140 ms, a rightward activation from 140 to 160 ms, and finally a posterior-leftward activation that ends at 192 ms.

The ECGsim isochrone map and CardioSynchroGram for the RBBB simulation is shown in fig. 2 panel C. The QRS duration was 184 ms, with earliest activation time on the ECGsim heart model at 8 ms (LV endocardium), and latest at 192 ms (RV lateral base). Septal activation was complete at 107 ms which is concurrent with the anterior LV wall (105 ms). The main part of the right ventricle is activated at 153 ms, with the right base being the only active part during the remainder of the QRS duration. On the CardioSynchroGram, there is a posterior-leftward activation until 102 ms. Thereafter, the direction is anterior (-right) with one area activating from 102 to 150 ms, and another from 156 ms to 170 ms.

Simulation of Spatially Confined Local Delays

For all nine cases with simulated activation delays, an additional colored cluster appeared on the CardioSynchroGram. Three examples of activation delays are illustrated in fig. 3, where the isochrone map from ECGsim is shown together with the transverse plane of the CardioSynchroGram. The onset and offset of the extra cluster are marked with a black arrow, and the weighted average is marked by a red dot. The

weights are the most negative slope (marked by a white dot) for each sample. Panel A shows the simulated delay in the node closest to V1, panel B shows the simulated delay in the node closest to V2, and panel C shows the simulated delay in the node closest to V6. Measurements for all nine simulated delays are given in table 1. There was no statistical difference between times set in ECGsim, and times measured using the CardioSynchroGram (mean \pm SD): 1.4 ± 3.8 ms (95% CI, -1.5 to 4.4, $p=0.29$).

Discussion

We derived the cardiosynchrogram, which indicates time and location for epicardial breakthrough of the heart. It is based on the 12-lead ECG and can therefore be used for both retrospective studies and in clinical settings.

Simulation of Gross Activation Patterns

Simulations of typical normal conduction, LBBB and RBBB show three distinct patterns in the cardiosynchrogram. In ECGsim, the following pattern is observed for normal conduction. The right ventricle shows first epicardial breakthrough, followed by the remaining free RV wall and the septum. Except for the right ventricular base, RV and septum are fully activated at 45 ms, whereas the LV free wall shows complete epicardial breakthrough at 61 ms. Thereafter, only the right base remains, which activates slowly for the remainder of the QRS duration. This corresponds with the pattern seen in the CardioSynchroGram, where first activation is seen in the right (-posterior) direction, and subsequently activation occurs in the leftward direction. After 62 ms, non-significant activation is seen, corresponding to the slow activation of the right base, which presumably has no effect on the pumping capacity of the heart. Hence, in this normal case, we interpret the two colored clusters of the cardiosynchrogram as representing firstly the right ventricle and septum, and secondly the left ventricle, as denoted on fig. 1C and fig. 2A. The remaining low-amplitude activation in the posterior-right direction may correspond to late basal activation, here denoted by “R Base” in fig. 1C and fig. 2A

For the case of LBBB, the same correspondence exists between isochrone maps and the CardioSynchroGram. The right ventricular free wall has initial epicardial breakthrough followed by complete septal breakthrough. Then activation transitions to the left ventricle, only 'disrupted' by the right base which has a late epicardial breakthrough. In this interval, the direction changes from posterior-left to right and back again, consistent with the isochrone map. Figure 2B was annotated according to this.

Also for RBBB the pattern seen on the CardioSynchroGram is consistent with the isochrone map obtained from ECGsim.

Simulation of Spatially Confined Local Delays

There was also a convincing agreement between simulated activation delays and EpiTimes measured based on the CardioSynchroGram. In fact, this holds not only for the temporal relation, but also for the spatial relation. As can be seen in figure 3, the location of the local delays shown by the CardioSynchroGram all correspond within 10 degrees to the position that was targeted in ECGsim.

Both temporal and spatial precision is higher for areas that activate in solitude, as opposed to e.g. a delayed activation occurring simultaneously with the main LV free wall. This is expected, since the CardioSynchroGram does not try to solve the inverse problem; it is merely a different visualization of the standard clinical 12-lead ECG.

General discussion

Due to the projection of the VCG on the defined lead vectors, clusters will always have a spread of 180° in the CardioSynchroGram. At all time points, we mark the dominant direction with a white dot for easy identification. In principle, only visualization of this "cell" would be necessary, however, the visual interpretation of the clusters that appear on the CardioSynchroGram is quite strong, and therefore we have maintained them in their entirety. The three planes visualized in the CardioSynchroGram may show different dyssynchronies. This is to be expected, as the activation of the heart is not necessarily symmetric

in the three planes. Most often, two planes will show the same dyssynchrony, and this will be the two planes that visualize the most dominant direction of activation (there is one direction in common between any pair of planes). This dominant direction should be used when assessing dyssynchrony, and it will normally be seen in the transverse plane.

Validating the CardioSynchroGram experimentally is quite difficult. Studies in animal models have simultaneously recorded epicardial potentials and body surface potentials [15], and in humans epicardial potentials were recorded [16], however with neither a 12-lead ECG nor body surface potential mapping. Similar setups could be used to compare measured epicardial breakthrough to EpiTimes obtained from the CardioSynchroGram.

The CardioSynchroGram may be applied retrospectively to conduct epidemiological studies on CRT. Such studies have been initiated to explore if there is correlation between dyssynchrony as measured by EpiTime on the CardioSynchroGram and survival in CRT patients.

Conclusion

This simulation study shows that the CardioSynchroGram gives an accurate description of electrical ventricular activation. Our findings also highlight the fact that QRS duration does not reflect local activation delays. Based on both the qualitative and quantitative results presented here, the CardioSynchroGram is a promising tool for visualization and quantification of ventricular dyssynchrony and the clinical value of these findings in cardiac resynchronization therapy is currently under investigation.

References

- [1] J. G. Cleland *et al.*, “An individual patient meta-analysis of five randomized trials assessing the effects of cardiac resynchronization therapy on morbidity and mortality in patients with symptomatic heart failure,” *Eur. Heart J.*, vol. 34, no. 46, pp. 3547–3556, Dec. 2013.
- [2] F. Tabrizi, A. Englund, M. Rosenqvist, L. Wallentin, and U. Stenestrand, “Influence of left bundle branch block on long-term mortality in a population with heart failure,” *Eur. Heart J.*, vol. 28, no. 20, pp. 2449–2455, Jul. 2007.
- [3] B. Surawicz, R. Childers, B. J. Deal, and L. S. Gettes, “AHA/ACCF/HRS recommendations for the standardization and interpretation of the electrocardiogram: Part III: Intraventricular conduction disturbances: A scientific statement from the American Heart Association Electrocardiography and Arrhythmias Committee,” *Circulation*, vol. 119, no. 10, pp. e235–e240, Mar. 2009.
- [4] P. Ponikowski *et al.*, “2016 ESC Guidelines for the diagnosis and treatment of acute and chronic heart failure: The Task Force for the diagnosis and treatment of acute and chronic heart failure of the European Society of Cardiology (ESC) Developed with the special contribution of the Heart Failure Association (HFA) of the ESC,” *Eur. Heart J.*, vol. 37, no. 27, pp. 2129–2200, May 2016.
- [5] C. W. Yancy *et al.*, “2013 ACCF/AHA Guideline for the Management of Heart Failure,” *J. Am. Coll. Cardiol.*, vol. 62, no. 16, pp. e147–e239, Oct. 2013.
- [6] C. Ypenburg *et al.*, “Long-Term Prognosis After Cardiac Resynchronization Therapy Is Related to the Extent of Left Ventricular Reverse Remodeling at Midterm Follow-Up,” *J. Am. Coll. Cardiol.*, vol. 53, no. 6, pp. 483–490, Feb. 2009.
- [7] E. B. Engels, M. Mafi-Rad, A. M. W. van Stipdonk, K. Vernooij, and F. W. Prinzen, “Why QRS Duration Should Be Replaced by Better Measures of Electrical Activation to Improve Patient Selection for Cardiac Resynchronization Therapy,” *J. Cardiovasc. Transl. Res.*, vol. 9, no. 4, pp. 257–265, 2016.

- [8] C. Ramanathan, P. Jia, R. Ghanem, K. Ryu, and Y. Rudy, "Activation and repolarization of the normal human heart under complete physiological conditions," *Proc. Natl. Acad. Sci.*, vol. 103, no. 16, pp. 6309–6314, Apr. 2006.
- [9] F. Del-Carpio Munoz *et al.*, "Delayed intrinsicoid deflection onset in surface ECG lateral leads predicts left ventricular reverse remodeling after cardiac resynchronization therapy," *Hear. Rhythm*, vol. 10, no. 7, pp. 979–987, Jul. 2013.
- [10] T. Lewis and M. A. Rothschild, "The Excitatory Process in the Dog's Heart. Part II. The Ventricles," *Philos. Trans. R. Soc. B Biol. Sci.*, vol. 206, no. 325–334, pp. 181–226, Jan. 2006.
- [11] L. Edenbrandt and O. Pahlm, "Vectorcardiogram synthesized from a 12-lead ECG: superiority of the inverse Dower matrix.," *J. Electrocardiol.*, vol. 21, no. 4, pp. 361–367, 1988.
- [12] J. A. Kors, G. Van Herpen, A. C. Sittig, and J. H. Van Bommel, "Reconstruction of the frank vectorcardiogram from standard electrocardiographic leads: Diagnostic comparison of different methods," *Eur. Heart J.*, vol. 11, no. 12, pp. 1083–1092, Dec. 1990.
- [13] A. van Oosterom and T. F. Oostendorp, "ECGSIM: an interactive tool for studying the genesis of QRST waveforms," *Heart*, vol. 90, no. 2, pp. 165–168, Feb. 2004.
- [14] G. Huiskamp and A. van Oosterom, "The depolarization sequence of the human heart surface computed from measured body surface potentials," *IEEE Trans. Biomed. Eng.*, vol. 35, no. 12, pp. 1047–1058, 1988.
- [15] L. R. Bear *et al.*, "How Accurate Is Inverse Electrocardiographic Mapping?," *Circ. Arrhythmia Electrophysiol.*, vol. 11, no. 5, p. e006108, May 2018.
- [16] M. Orini, P. Taggart, N. Srinivasan, M. Hayward, and P. D. Lambiase, "Interactions between Activation and Repolarization Restitution Properties in the Intact Human Heart: In-Vivo Whole-Heart Data and Mathematical Description," *PLoS One*, vol. 11, no. 9, p. e0161765, Sep. 2016.

Journal Pre-proof

Table 1:

	Activation time [ms]								
	V1	V2	V3	V4	V5	V6	Sep. Base	Inf. LV	Sup. LV
ECGsim	93	82	64	72	64	82	68	70	75
EpiTime	95	77	69	71	71	79	71	73	77

Journal Pre-proof

Captions

Table 1: Activation times from ECGsim and EpiTimes obtained from the Cardiosynchrogram. All values are relative to QRS onset.

Figure 1: Panel A shows a stylistic presentation of the activation sequence of the heart, and how it gives rise to the ordinarily known ECG. Panel B shows the basic steps in creating a cardiosynchrogram: an ECG (leads V1-V6 shown here), the first derivative of the same ECG, and the direct precordial CardioSynchroGram. It is obtained by making a colored band for each lead, and color coding it according to the following scheme. Positive derivative values are colored white, whereas negative derivative values are colored from yellow to blue as the derivative becomes larger (more negative). Panel C shows the CardioSynchroGram from 36 virtual leads in each plane (transverse, frontal and sagittal). The vectorcardiogram (VCG) is computed by inverse Dower or Kors transforms, and is then projected onto every of the defined virtual leads to obtain the “ECG” of each lead. These ECGs are then differentiated, and the values shown as color-coded bands similarly to the precordial CardioSynchroGram.

Figure 2: Panel A shows a simulation of the “normal male” of ECGsim. The isochrone map shows that the main right and left ventricle are activated after 60 ms, corresponding to the CardioSynchroGram. Thereafter, only the right base is active, because activation travels perpendicular to the nearest electrodes it shown only as a light yellow color.

Panel B shows the case of LBBB as described in detail in the text. Here, right ventricle and septum activates first with epicardial breakthroughs until 90 ms, thereafter the left ventricle takes over. From 140 to 160 ms the right base depolarizes, causing a deflection in the direction towards right. Thereafter the direction is left again, corresponding to LV free wall.

Panel C shows RBBB. Activation starts in the left ventricle, but in a postero-right direction. The activation front then moves towards the anterior left and through septum, until both are activated at 100 ms. The

right ventricle activates in an anterior direction ending more towards right (note the orientation of the heart). Finally, the propagation through the right base is more towards the right.

In both panel B and C, the position of RV and LV is changed with respect to panel A. This change in RV and LV position on the CSG is due to a more uniform activation along in the RV-LV axis in both LBBB and RBBB compared to normal activation, where there is also an apicobasal component.

Figure 3: Typical examples of spatially confined local activation delays. Panel A shows the simulated delay below V1, panel B shows the simulated delay below V2, and panel C shows the simulated delay below V6. For all delays, there is a clear and distinct cluster in addition to the two main clusters denoting right and left ventricle. The direction of these clusters correspond with the delayed areas. EpiTime is computed as the weighted average time of the cluster.

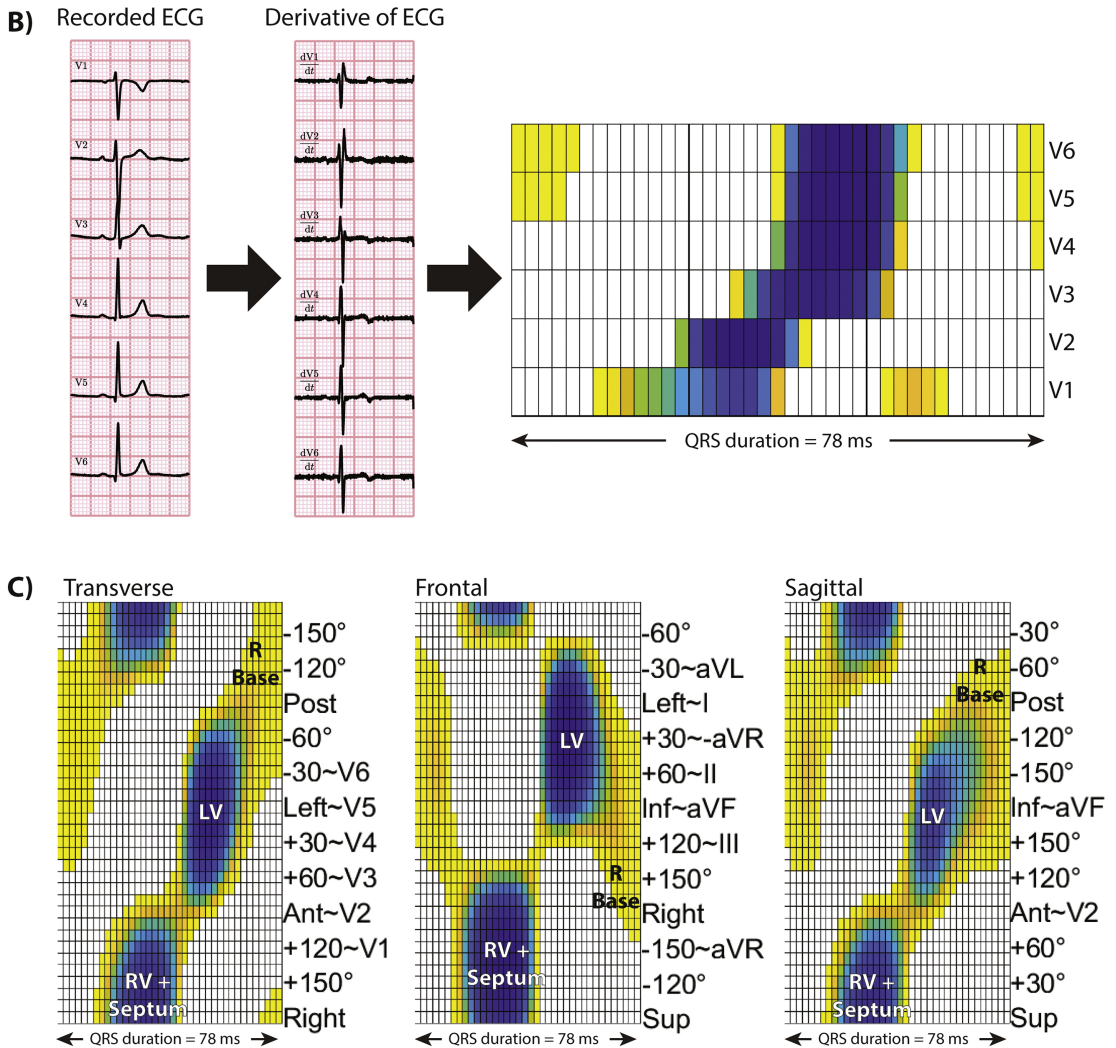
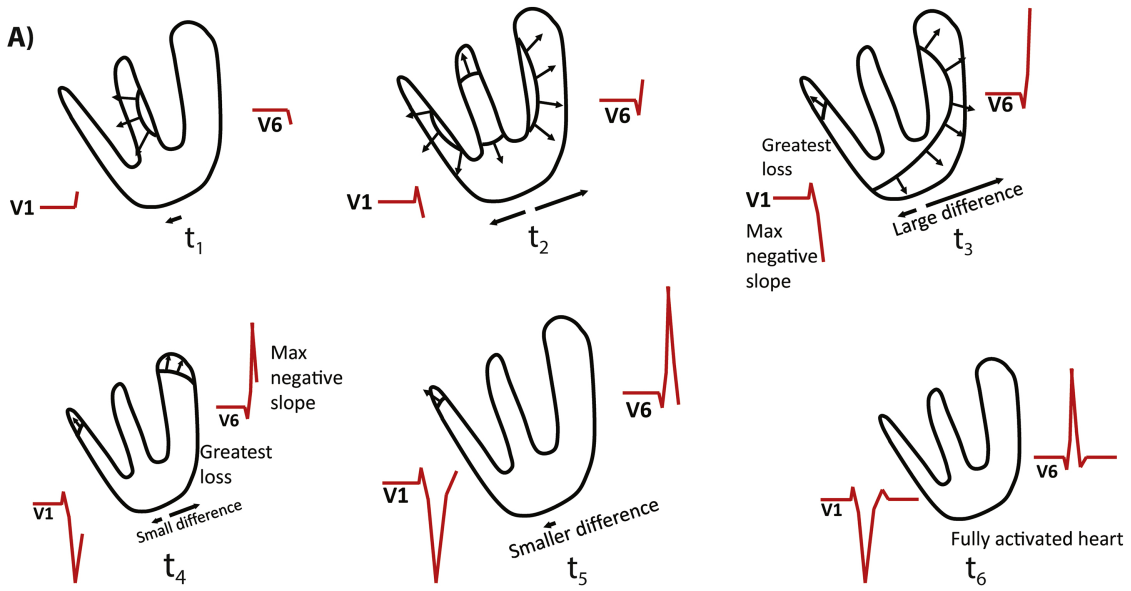


Figure 1

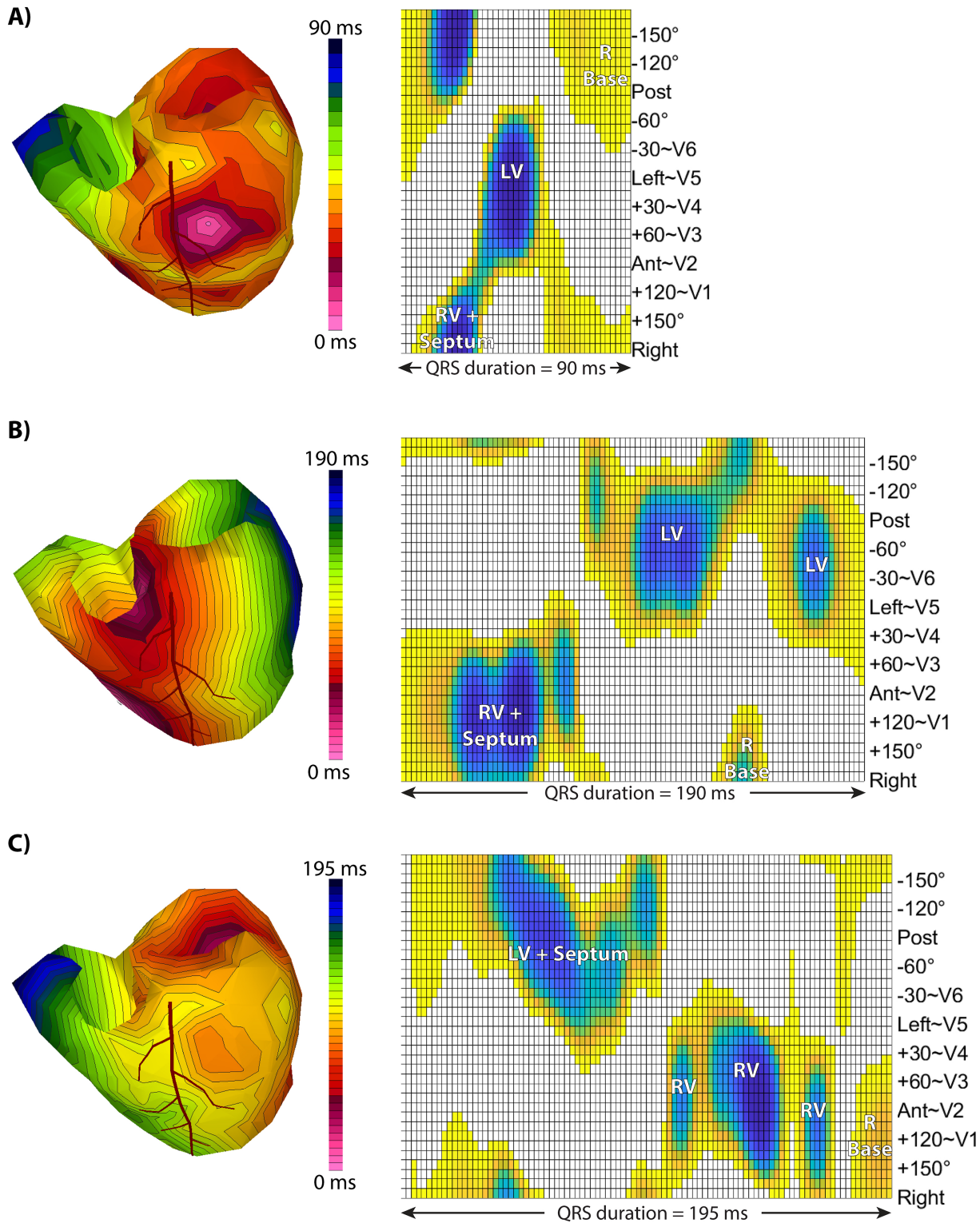
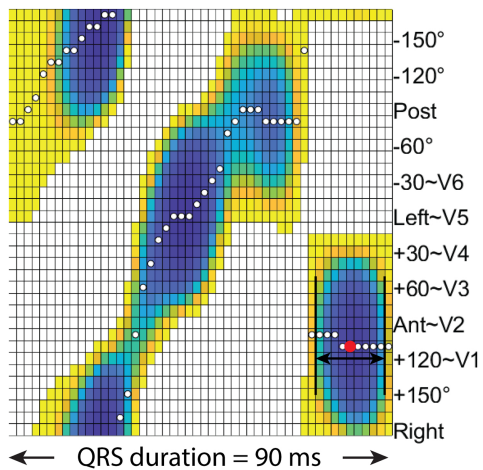
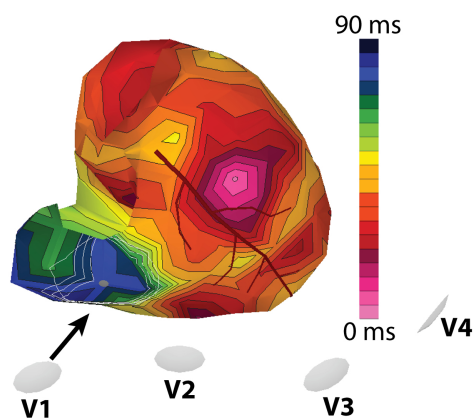
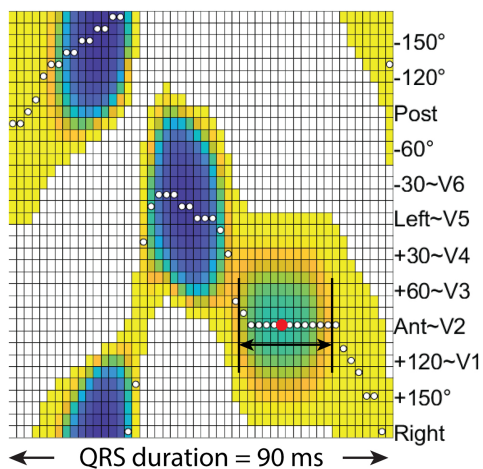
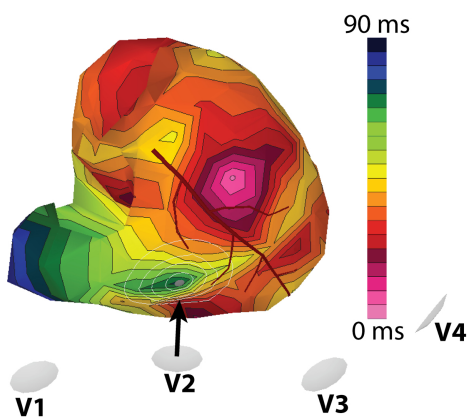


Figure 2

A)



B)



C)

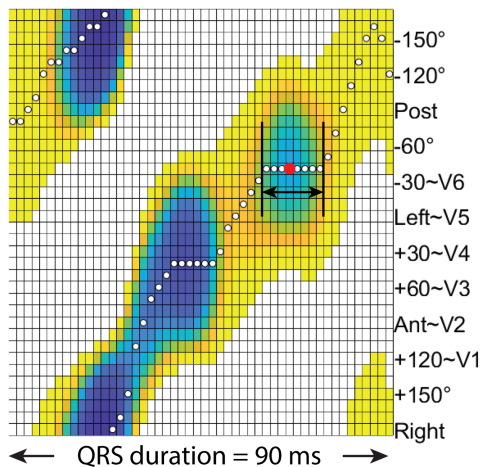
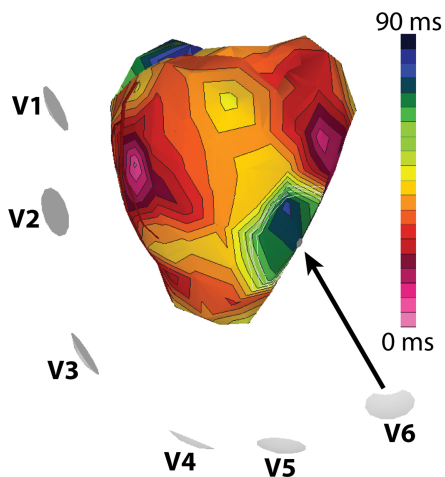


Figure 3